

CAD modelling of the chip shape in case of ball-end milling

Bálint Varga^{a,b*}, Balázs Mikó^a

^a Óbuda University, Doctoral School on Materials Sciences and Technologies

^b Óbuda University, Institute of Material and Manufacturing Science

ABSTRACT

The manufacturing of free form surfaces is a common task in the field of mould and die manufacturing. The changing circumstances of the finishing milling with ball-end milling cutter has effect on the shape and the volume of the chip, the load of the cutting tool and the generated surface roughness. The aim of the article is to investigate the changing of the chip thickness and volume in case of ball-end milling by 3D CAD modelling, and to analyse the changing of the circumstances in case of milling of a convex and a concave surfaces.

Keywords: *free form surface, ball-end milling, chip, CAD modelling, average chip thickness*

1. Introduction

In injection moulding tools, dies or in the manufacture of vehicle bodies, free-form surfaces are also encountered, and machining them requires high precision as well as productivity. In the field of mold and die production, these surfaces are basically made by milling, where finishing is done by a ball-end mill. During milling of a free-form surface with a ball-end mill, depending on the nature of the surface, the working edge section, the working diameter and thus the cutting conditions, the shape and volume of the chip, and the cutting force change continuously [1, 2]. This affects the load on the tool, the quality of the resulting surface, and the wear of the tool.

The volume of the chip in the case of milling can be determined as the multiplication of the cutting depth (a_p), the cutting width (a_e) and the cutting feed (f_z):

$$V_c = a_p \cdot a_e \cdot f_z. \quad (1)$$

However, during machining with a ball end mill, the depth of cut and width of cut values differ from the nominal values due to the mentioned conditions. There are several methods for determining the shape and the volume of a chip.

Analytical description of the tool edge and surface enables the exact description of the chip shape, however, due to the consideration of the surface description and the tool edge, it requires complicated calculations [3, 4]. The volume of the chip can also be determined as the product of the feed per tooth and the orthogonal area of the chipped area [5]. This cutted surface segment can also be produced with a simplified geometrical description of the ball-end tool [6]. The variable location and size of this surface determines the required power, dynamic conditions, and surface roughness of machining with a ball end mill [2].

In addition to the analytical and geometric description, the chip shape can also be examined with CAD modelling [7]. The chip removal is simulated in a 3D virtual environment. The aim of

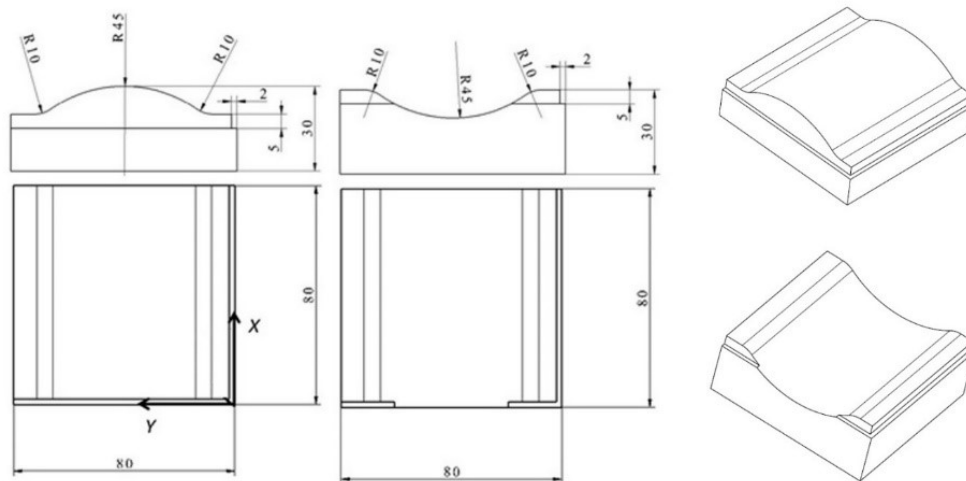


Figure 1. Geometric design of the test part

the research is to investigate the accuracy of surfaces machined with a ball-end mill, primarily to investigate the relationship between milling strategy and shape accuracy [8, 9]. The purpose of this is to be able to choose the appropriate milling strategy, taking into account the micro- and macro-accuracy of the surface, and to determine its technological and geometric parameters when using CAM systems.

The purpose of this article is to determine the shape and cross-section of the chip removed during surface milling with a ball end mill using 3D geometric modelling, and to analyze the change in the cutting conditions.

2. Method

The size of the test part is $80 \times 80 \times 30$ mm, the tested free-form surface is a cylindrical surface with a radius of 45 mm. This surface is connected to the horizontal plane by a rounding with a radius of 10 mm. In order to examine the geometrical conditions, we also examined the geometry of convex and concave parts. The dimensions of the test part are shown in Fig. 1. The height and depth of the large cylindrical surface of the convex (convex - CX) and concave (concave - CV) part is 9.2 mm. The size of the test part was defined considering manufacturing and measuring aspects.

During the geometric modelling of the chip shape, the CATIA V5 CAD system was used. During the modelling, the factors influencing the chip shape were parameterized, so by changing them, the conditions of the chipping can be examined. The examined parameters are: the position (x, y) of the tool diameter (D_c), the surface normal, the tool feed (f_z), the feed direction (A_f), the cutting width (a_e) and the cutting depth (a_p).

During the simulation, we changed the value of the feed per tooth and the width of cut with several feed directions. The tool diameter was $D_c = 10$ mm, the cutting depth was $a_p = 0.3$ mm, and the direction of the surface normal is determined by the shape of the test piece and the current position of the tool.

Table 1. Cutting parameters

Parameter	1	2	3	4	5
f_z [mm]	0.08	0.08	0.08	0.12	0.16
a_e [mm]	0.35	0.25	0.15	0.15	0.15

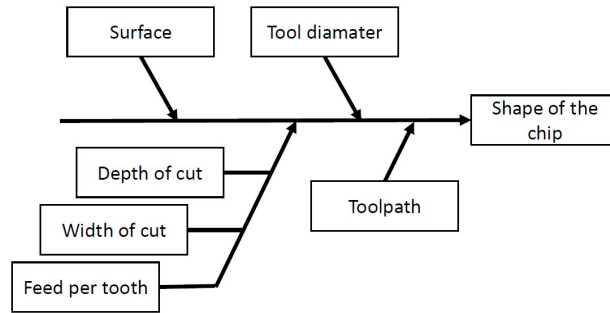


Figure 2. Factors determining the shape of a chip

Based on the CAD model, the volume (V) of the generated theoretical chip shape was determined, as well as the average chip thickness (h_m) as a quotient of the volume and the surface area (A) facing the direction of the tool. The values of the feed direction during modelling were 0.0° , 22.5° , 45.0° , 67.5° and 90.0° . The values of feed and width of cut were examined in 5 sets according to [Table 1](#).

3. CAD modeling of the chip

During the geometric modelling, the goal was to create a parametric CAD model, which is suitable for determining the volume and cross-section of the resulting chip at any point of the surface model. For this, it is necessary to parameterize the tool position coordinates, as well as to consider additional parameters that determine the shape of the chip. These parameters are the depth of cut (a_p), the lateral step (width of cut) (a_e), the feed per tooth (f_z), the angle of the milling direction (A_f) and the diameter of the tool (D_c) ([Fig. 2](#)). The modelling method focuses only the geometric circumstances, and cannot consider the effect of the tool edge geometry, the cutting speed and the mechanical properties of the workpiece and the tool. The modelling process was demonstrated on the convex piece. The modelling was performed at a thousandfold magnification due to the geometric resolution of the CAD system. The first step of the modelling is to shift the initial surface by the value of the depth of the cut (a_p), which represents the pre-smoothed geometry ([Fig. 3](#)). The next step

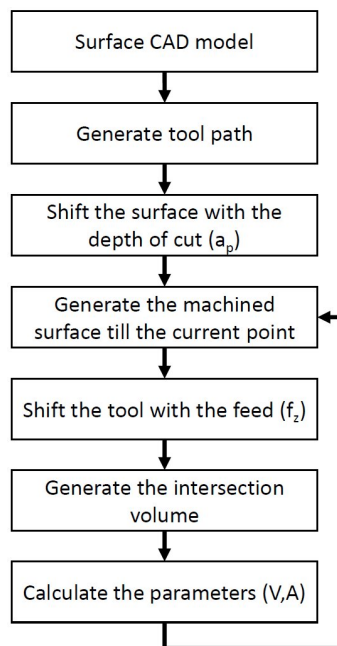


Figure 3. The modelling process

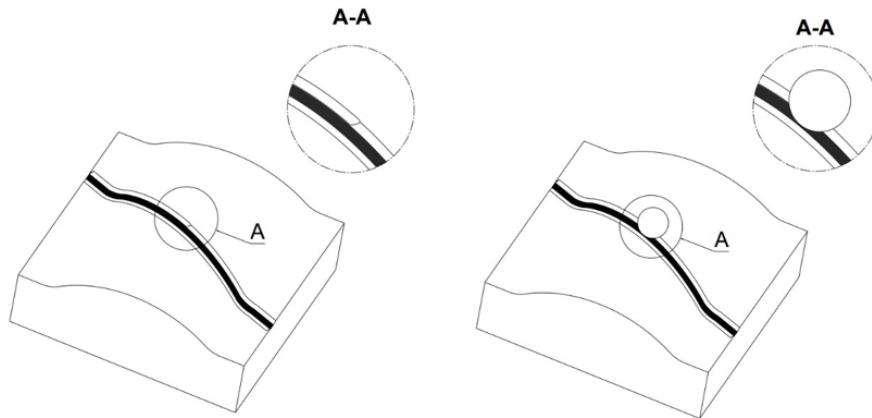


Figure 4. CAD model of the simulation

of the modelling is to parameterize the coordinate points of the toolpath. A hemisphere of a given diameter, representing the cutting tool, is traced along the toolpath constructed on the surface, thus touching the surface that is to be machined. The part of the material that has already been touched by the tool must then be removed up to the coordinate where the shape and parameters of the chip are determined (Fig. 4).

The figure on the left shows the surface already machined at the given coordinate. On the right, the same is shown with a symbolic representation of the tool in the tested position. The tool, i.e. the hemisphere, is offset along the toolpath by exactly the same amount as the feed per tooth. In the presented picture, not all toolpaths are visible due to the graphics capability of the computer, only the 20 toolpaths before the measuring point are shown, which are visible as a thick black line. This simplification does not affect the result. In the final step, only the common part of the two bodies, the tool and the machined surface, is created, resulting in the geometric model of the chip shown in Fig. 5.

The test involved modelling the chips at 21 points on both workpieces. At these points, the surface normal is always in a different direction, varying continuously from 0° to 33° in one direction (y) only, due to the surface to be machined. The positions of the test points are shown in Fig. 6. A total of 1050 chip shapes were defined in the modeling.

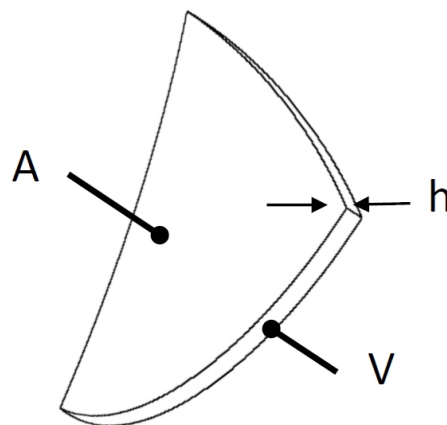


Figure 5. Modelled chip shape

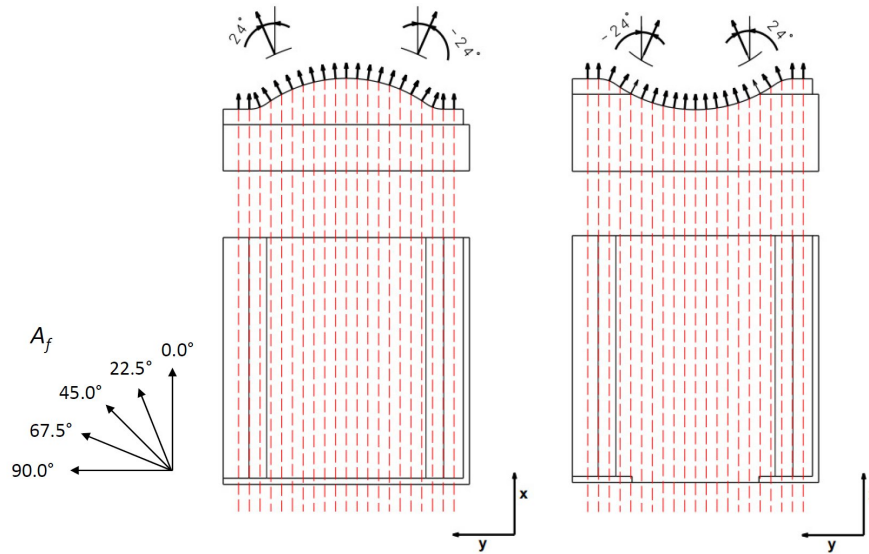


Figure 6. Tool positions investigated in the modelling

4. Results

The CAD simulation of the chip removal shows that the chip volume and chip thickness change along the path due to surface variation, and that this variation is different for the concave (CV) and convex (CX) pieces. At the horizontal sections (points 1 and 21), the chip volume is equal to the theoretical value given by Eq. (1). Fig. 7 shows the variation for the parameters at $f_z = 0.12$ mm and $a_e = 0.15$ mm.

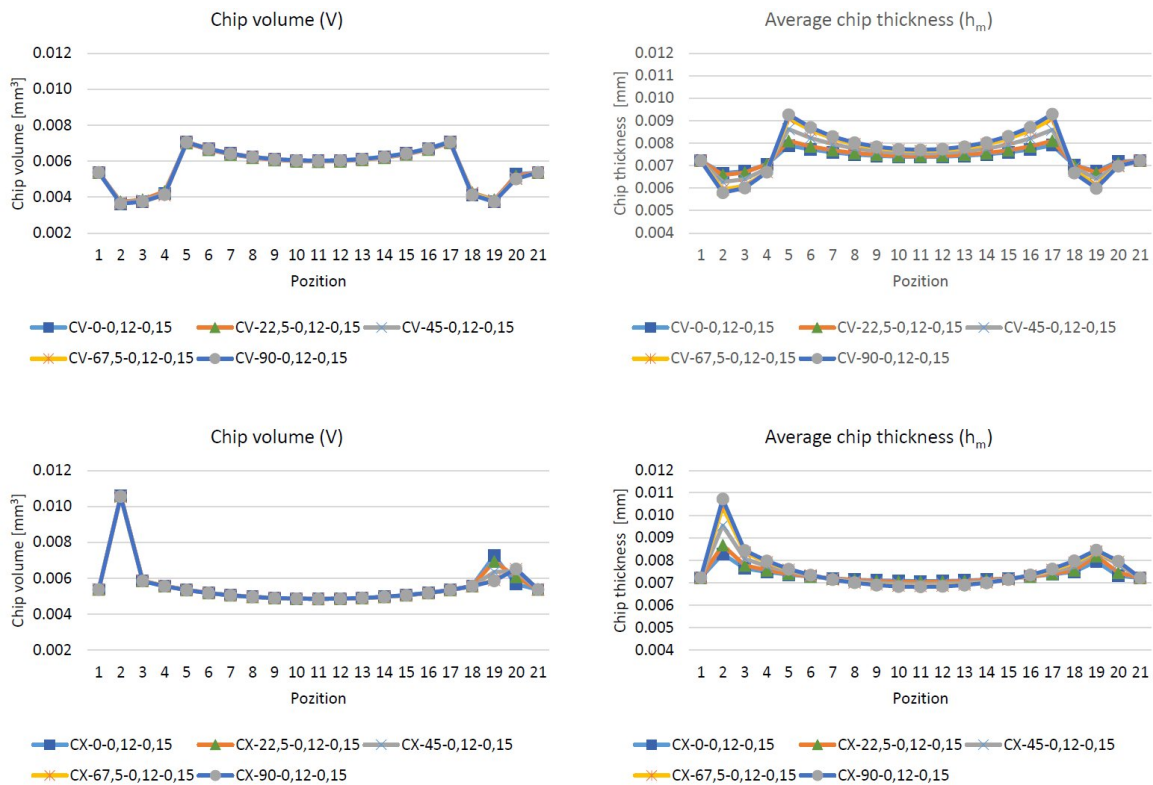


Figure 7. Variation of chip volume and mean chip thickness as a function of milling direction

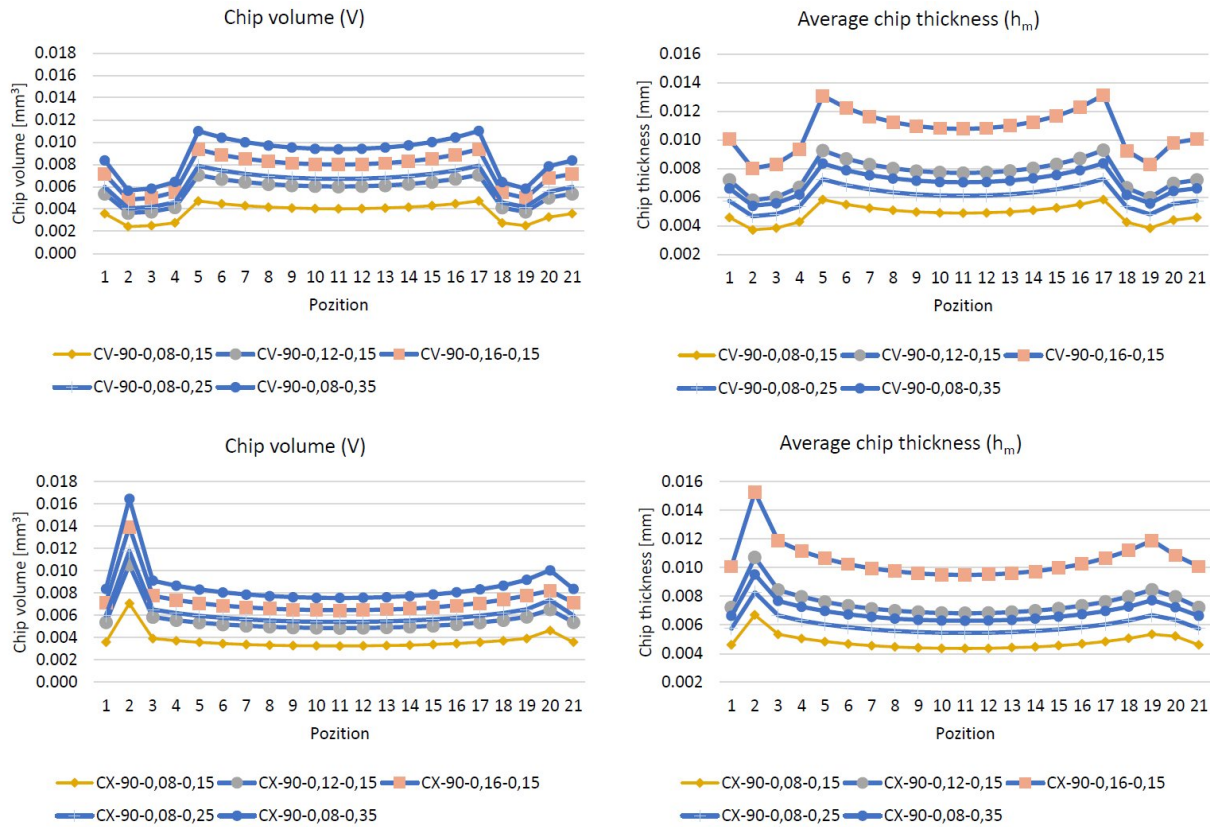


Figure 8. Variation of chip volume and mean chip thickness as a function of milling parameters for 90° milling direction

The nature of the curves is different at convex and concave surfaces, as more of the tool is in contact with the surface when milling a concave surface. For concave surfaces, the chip volume is larger on the R45 curved section. As can be seen, the chip volume and chip thickness curves are not symmetric, so the chip volume and mean thickness are different in the straight and curved (R10) sections of the inlet and outlet. In the case of a concave (CV) surface, the inlet and outlet radius is convex, reducing the chip volume. For the convex surface (CX), the radius is concave, so there is a large increase. The rate of increase depends on the relationship between the surface radius and the tool radius. The increase is smaller at the outlet section. Since a different section of the tool contacts the surface on either side of the test surface, the volume of the chip is also different.

For the chip volume, the curves are nearly coincident, so the value does not depend on the milling feed direction. However, the values for the mean chip thickness differ, so the milling direction affects its value. The diagram shows that the mean chip cross-section is smallest at $A_f = 0$ and largest at $A_f = 90$. The deviation is smaller for the convex (CX) surface.

The effect of feed per tooth and width of cut is shown in Fig. 8 for a 90° milling direction. As can be seen, the curves are similar. The smallest chip volume there is at $f_z = 0.08$ mm, $a_e = 0.15$ mm, the largest at $f_z = 0.08$ mm, $a_e = 0.35$ mm, so the role of the width of cut (a_e) is more important. The average chip thickness there is at $f_z = 0.16$ mm, $a_e = 0.15$ mm, where the feed per tooth (f_z) plays a more important role.

Further tests will only analyse data for the R45 mm curved section. Fig. 9 shows the average values of the simulations with the given parameters f_z and a_e . They show that in case of the concave (CV) surface, both chip volume and mean chip thickness are larger. In the case of volume, the width of cut has a greater effect, and in the case of chip thickness, the feed rate has a greater effect.

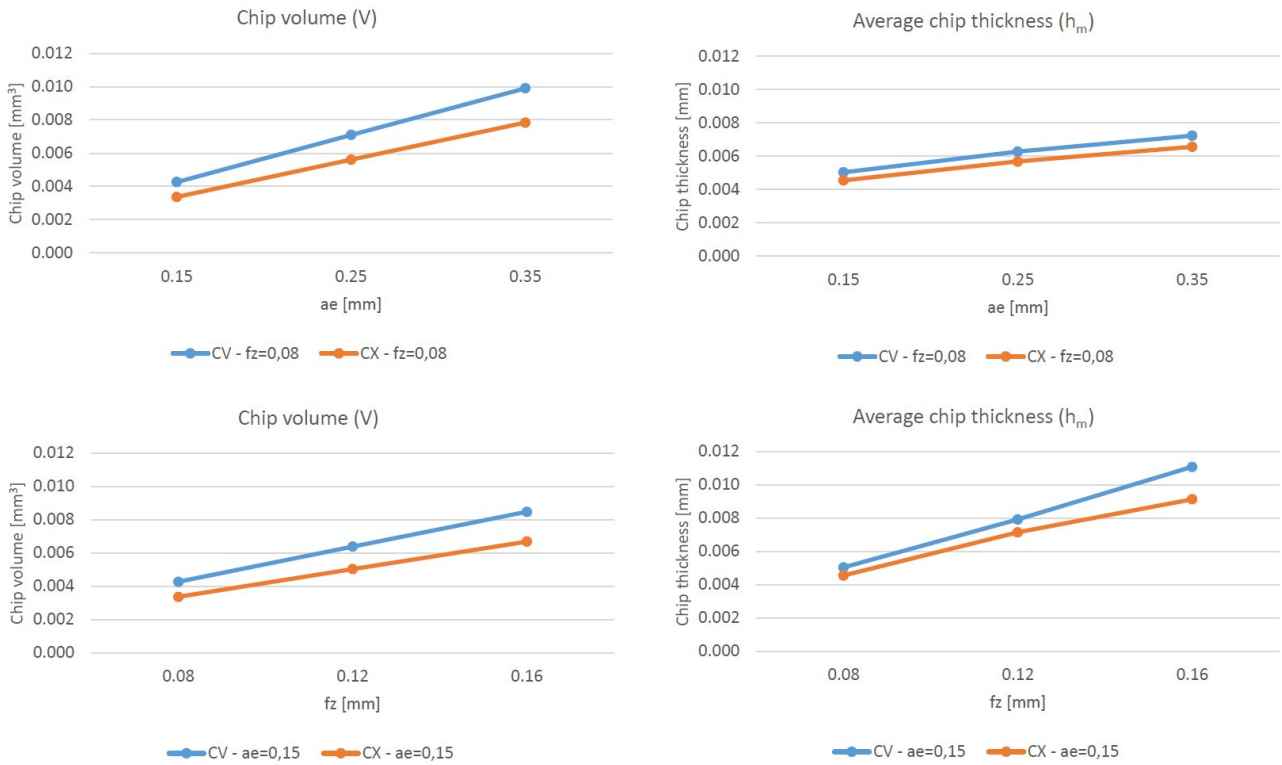


Figure 9. Average values on the curved (R45) section

Fig. 10 and 11 show the average values for milling with the given parameters in the given direction. They show that the average value of the chip volume is not sensitive to the milling direction and higher for concave surfaces. The value of the standard deviation, which indicates the variation along

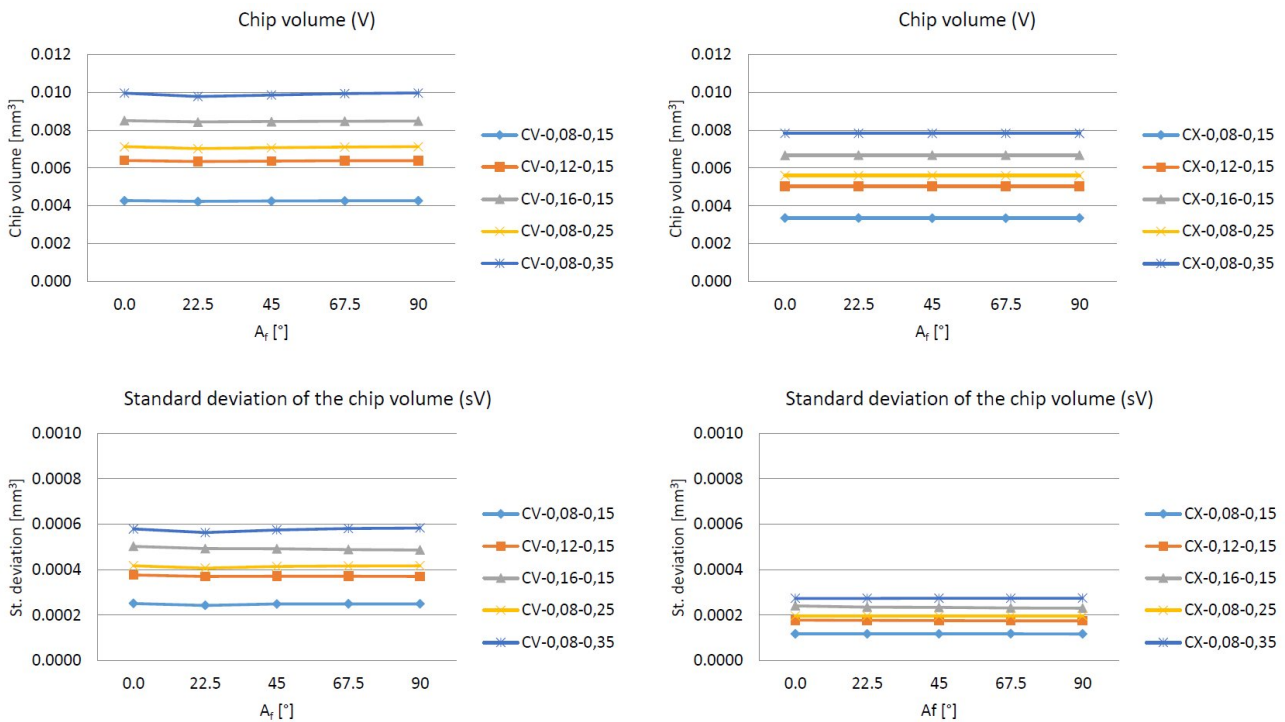


Figure 10. Mean and standard deviation of chip volume by milling direction

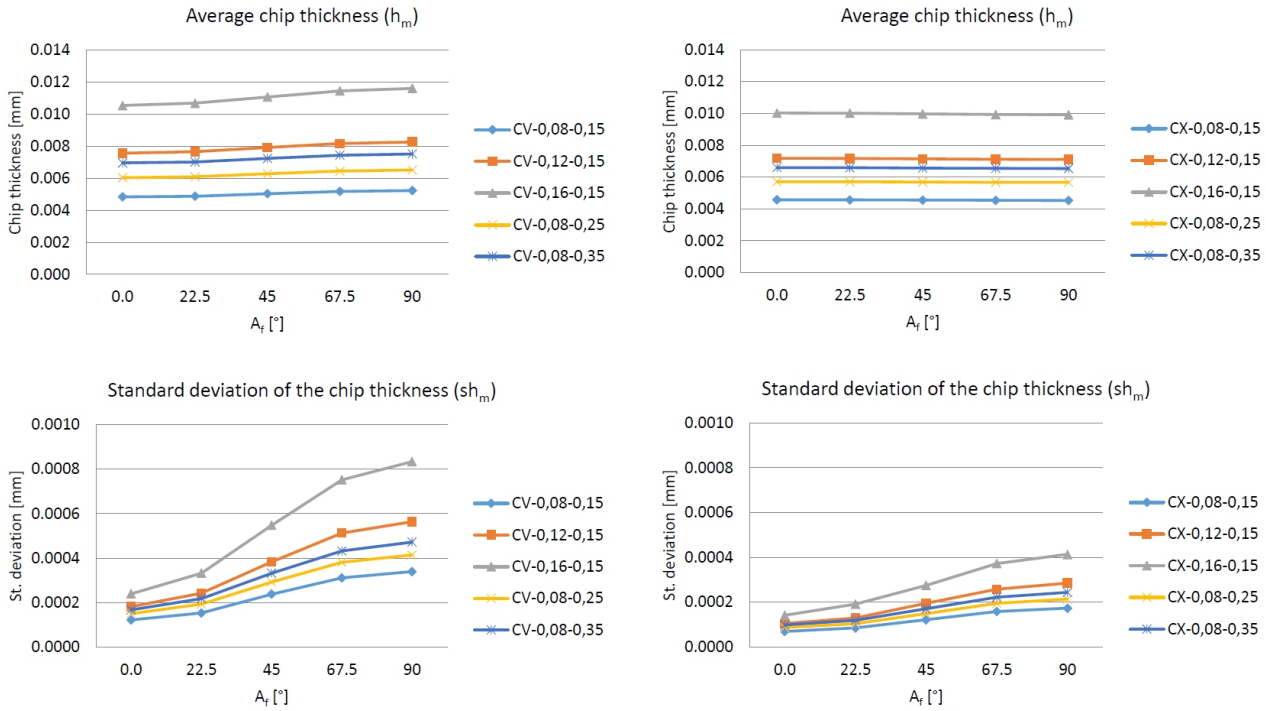


Figure 11. Mean and standard deviation of average chip thickness by milling direction at R45

the path, is also insensitive to the milling direction, being larger for concave (CV) surfaces and smaller for convex surfaces (CX), i.e. the chip volume varies less along the path for convex surfaces. The average values of the mean chip thickness (Fig. 11) show a small increase with the change in milling direction for the concave (CV) surface, while there is no effect when milling the convex surface. On the other hand, the standard deviation values of the mean chip thickness along the tool path vary significantly with the direction of the path, with the smallest variation at 0° and the largest variation at 90°. The variation is larger for a concave surface than for a convex surface.

5. Conclusions

When finishing a free-form surface with a ball-end milling cutter, the conditions of chip removal are constantly changing as the surface changes, affecting the tool load and the micro and macro accuracy of the surface. In case of concave and a convex free-form surfaces machined with a ball-end milling cutter, the shape, volume and average thickness of the chip were investigated by CAD simulation.

Based on the simulations, it was found that (1) the theoretical turning volume agrees with the simulation values only in the horizontal sections; (2) for concave and convex surfaces, the chip volume and mean thickness vary differently; (3) for concave pieces, the chip volume is larger under the same conditions; (4) for chip volume, the width of cut has a greater effect, for chip thickness, the feed rate has a greater effect; (5) the mean value and variance of the chip volume are not sensitive to the milling direction; (6) the average value of the mean chip thickness is only slightly sensitive to the milling direction, but the variation along the path (standard deviation) is significant. The presented method also provides the possibility to study the tool load variation, to select the appropriate milling strategy and to determine the theoretical roughness.

6. References

- [1] T. Altan, B Lilly, Y.C. Yan, *Manufacturing of dies and moulds*, CIRP Annals - Manufacturing Technology 50(2), 2001, pp. 404-422, [CrossRef](#)
- [2] C.K. Toh, *A study of the effects of cutter path strategies and orientations in milling*, Journal of Materials Processing Technology 152, 2004, pp. 346–356, [CrossRef](#)
- [3] L. Sai, R. Belguith, M. Baili, G. Dessenin, W. Bouzid, *An approach to modelling the chip thickness and cutter workpiece engagement region in 3 and 5 axis ball end milling*, Journal of Manufacturing Processes 34 A, 2018, pp. 7–17, [CrossRef](#)
- [4] L. Sai, R. Belguith, M. Baili, G. Dessenin, W. Bouzid, *Cutter-workpiece engagement calculation in 3-axis ball end milling considering cutter runout*, Journal of Manufacturing Processes 41, 2019, pp. 74–82, [CrossRef](#)
- [5] T. Huang, X. Zhang, H. Ding, *Decoupled chip thickness calculation model for cutting force prediction in five-axis ball-end milling*, The International Journal of Advanced Manufacturing Technology volume 69, 2013, pp. 203-1217, [CrossRef](#)
- [6] A.F. de Souza, A.E. Diniz, A.R. Rodrigues, R.T. Coelho, *Investigating the cutting phenomena in free-form milling using a ball-end cutting tool for die and mold manufacturing*, The International Journal of Advanced Manufacturing Technology 71, 2014, pp. 565–1577, [CrossRef](#)
- [7] H. Iwabe, K. Shimizu, M. Sasaki, *Analysis of cutting mechanism by ball end mill using 3D-CAD*, JSME International Journal Series C 49(1), 2006, pp. 28-34, [CrossRef](#)
- [8] B. Mikó, B. Varga, W. Zebala, *The effect of the feed direction on the micro- and macro accuracy of 3D ball-end milling of chromium-molybdenum alloy steel*, Materials 12, 2019, 4038, [CrossRef](#)
- [9] B. Varga, B. Mikó, *Impact of different CAM strategies and cutting parameters on machining free-form surfaces with ball-end milling tool in terms of micro and macro accuracy*, Acta Polytechnica Hungarica 18(7), 2021, pp. 109-128, [CrossRef](#)